Crosslinked graphene oxide membranes: enhancing membrane material conservation and optimisation

Vepika Kandjou[a,b], Miguel Hernaez[a], Maria D. Casal[c] and Sonia Melendi-Espina[a*]

[a]*School of Engineering, University of East Anglia (UEA), Norwich Research Park, NR4 7TJ, Norwich, United Kingdom*

[b]*Department of Chemical, Materials and Metallurgical Engineering, Botswana International University of Science and Technology (BIUST), P/Bag 16, Palapye, Botswana*

[c]*Instituto de Ciencia y Tecnología del Carbono (INCAR-CSIC), c/ Francisco Pintado Fe 26, 33011, Oviedo, Spain*

GRAPHICAL ABSTRACT

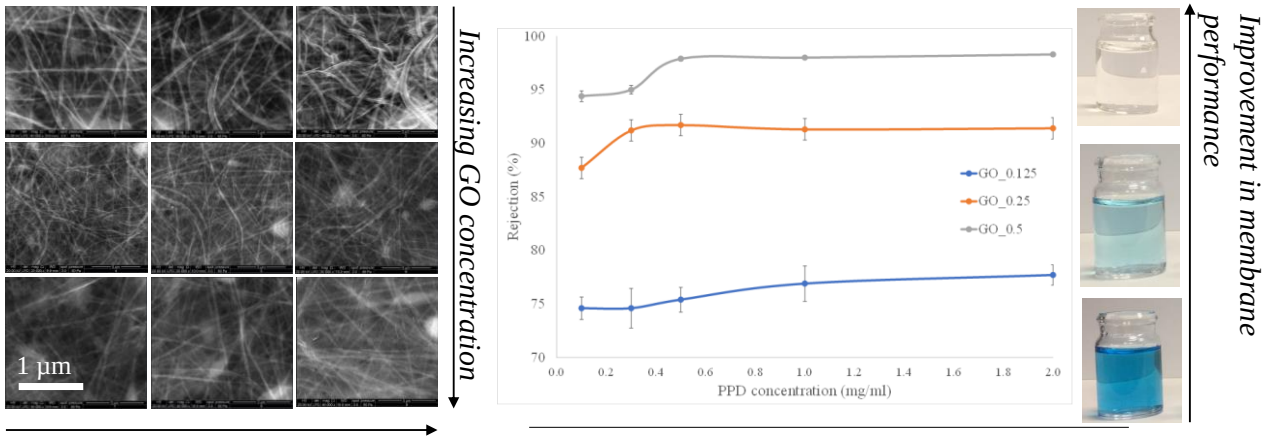

SEM of fabricated membranes at different concentrations

ABSTRACT

Background: Graphene Oxide (GO) has recently shown great promise in water purification as a potential substitute to conventional membrane materials. However, GO membranes face some

Corresponding author: Sonia Melendi-Espina; s.melendi-espina@uea.ac.uk (Tel: +441603592848)

challenges associated to their swelling due to the accumulation of water molecules in their oxidised regions. The use of crosslinkers has been proven as an effective way to improve GO membranes stability and performance. Nevertheless, optimisations to efficiently use materials and resources are a necessity. These include the determination of the influence of GO and crosslinker amounts on membrane structure, operation, and efficiency. **Methods:** Consequently, in this study crosslinked membranes with different GO and p-phenylenediamine (crosslinker) concentrations were fabricated to establish relationships between the quantity of the selected materials and membranes performance. FESEM was undertaken to investigate the structural quality together with thickness measurements. The performance of the membranes was evaluated via a pressure assisted nanofiltration cell using aqueous methylene blue (MB) as feed solution. **Significant findings**: A notable enhancement in MB separation from around 75% to 98% was observed at an increasing GO and crosslinker concentrations. The permeation flux decreased correspondingly owing to tortuosity lengthening at higher GO concentrations. Based on performance rates and XPS characterisations the optimum crosslinker and GO concentrations were deduced.

KEYWORDS

Graphene oxide, layer-by-layer, concentration, optimisation, crosslinking, nanofiltration

1. Introduction

The increasing global water stress and consumption demand alludes to the urgent need for the manufacturing of durable and efficient water purification materials and procedures [1–3]. Among the existing purification processes, like distillation, flocculation and coagulation, membrane separation is relatively the most favourable due to its reliability coupled with efficiency in contaminant removal and the variety of materials available for usage [4,5]. Often employed materials include polymers, such as poly (ether sulfone), nylon and polyethyleneimine [6,7], however their relatively low strength and increased vulnerability to bio-fouling calls for the consideration of alternative substitutes [6]. In this

context, the use of inorganic membrane materials like ceramics has been reported, but in some cases the limited permeability is noted as a hindrance [6].

Within this framework, graphene is considered a promising alternative, owing to its 2-dimentionality and remarkable mechanical strength [8]. Nevertheless, its lack of production scalability at a reasonable price along with the complex and cost-intensive pore formation process needed during membrane fabrication impedes its wide use as a membrane material [9–11]. Luckily, its derivative GO is an equitable alternative, as it can be fabricated economically in large quantities [12–15]. Structurally, GO amphiphilic nature also offers a unique quicker permeation tortuous route that allows un-impeded flow of water molecules while blocking other species [12]. Furthermore, the availability of oxygen functionalities enhances its ability to be dispersed in polar solvents. This gives it an applicative advantage over other carbonaceous materials, like carbon nanotubes (CNTs), since GO can be more easily processed to various useful devices [6,16].

Nonetheless, the presence of these oxygenated functional groups also brings a fundamental limitation of poor membrane stability during operation [17,18]. It has been highlighted and observed that GO membranes tend to swell in aqueous environments due to the accumulation of water molecules in its oxidised regions [17]. Numerous attempts have thus far been carried out to enhance GO membrane performance and stability [19,20]. For example, affordable p-phenylenediamine (PPD) has been successfully incorporated as crosslinker in GO membranes to significantly improve membrane performance and stability [21,22]. Physicochemical characteristics of GO, specifically the average lateral size, colloidal stability and surface chemistry also play a significant role on membrane fabrication and performance [23]. Few works also suggest that GO concentration seem to be an essential factor in controlling both fouling susceptibility and flux across GO membranes [24,25]. However, there is a lack of studies that evaluate the influence of GO and crosslinker concentrations on fundamental membrane characteristics, such as membrane morphology, homogeneity, and relative thickness, as well as integrity and overall membrane separation. Therefore, it is the aim of this work,

as this is essential in enhancing performance efficiency and promoting in this way a responsible use of resources [26]. Relevant characterisations from thickness measurements and X-ray Photoelectron Spectroscopy (XPS) to Field-Emission Scanning Electron Microscopy (FESEM) characterisations pre and post nanofiltration experiments were undertaken to determine homogeneity, surface intactness and stability.

2. Experimental section

2.1 Materials

GO powder was purchased from Graphenea (Spain) and used to prepare a range of suspensions with different concentrations. Polyacrylonitrile (PAN) substrates from Sterlitech Corporation (NY, USA) were employed as membrane supports. Glass slides purchased from Fisher Scientific (UK) were used to deposit alike crosslinked thin films for thickness quantification. For low GO concentrations (0.125 mg/ml) silicon wafers from Sigma Aldrich were used, as the roughness of the glass slides limited the accuracy of the measurements.

The GO membranes were crosslinked with PPD purchased from Sigma Aldrich, UK. Polyethyleneimine (PEI) and potassium hydroxide powder (KOH), which were used during membrane preparation, and methylene blue (MB) - used during nanofiltration - were all sourced from Sigma Aldrich (UK) as well.

2.2 Membrane assembly, characterisation and nanofiltration tests

GO aqueous suspensions of 0.125, 0.25 and 0.5 mg/ml and 0.1, 0.3, 0.5, 1.0 and 2.0 mg/ml solutions of PPD were prepared. To ensure suspension dispersibility, the respective GO samples were sonicated for 2 hours in a bath type sonicator with 280W sonication power from Fisherbrand, UK.

The membranes were fabricated with the aid of a rotary dip-coater (Nadetech, Spain). Details of the fabrication procedure of the membranes have been described in our previous work elsewhere [22].

Briefly, the substrates were pre-treated immersing them in 1M KOH to instigate a negative charge, and subsequently in a positively charged 2.0 mg/ml aqueous PEI solution with wash steps in between. Afterwards, substrates were introduced in the selected GO suspension for 1 min, rinsed in deionized water and dried, and subsequently immersed in the particular PPD solution. The washing and drying processes were also carried out after the dip in the crosslinker solution. This deposition routine was repeated 5 times to attain 5-bilayer membranes. The membranes were labelled using the notation GO_x.PPD_y, where *x* and *y* are the concentrations of GO suspension and PPD solution respectively. Results reliability was enhanced through fabricating and testing three membranes of each type at the respective concentrations.

The variation of membrane thickness with concentration was estimated using a Bruker DektakXT Profiling System (Stylus Profiler) through fabricating identical thin films onto glass slides or silicon wafers. Reliability was enhanced by taking an average of 10 measurements and recording the deviation from the average accordingly.

Surface chemistry of the fabricated membranes was studied by means of XPS, using a Kratos Axis Ultra-DLD, K-Alpha+ instrument. Wide scan spectra were obtained to identify the elements present on the membranes along with the high-resolution spectra to categorise and quantify the oxygen functional groups on the surface. Different peaks emerged in the C1s curve fitting, which correspond to C graphitic, C-OH hydroxyl/C-O-C epoxide, C=O carbonyl, COOH carboxyl groups along with the π-π* shake-up signal. Some of these peaks overlap with others attributed to nitrogen functionalities, specifically between C-O-C epoxide and C=N and between C=O and C-N [27–29].

Membrane homogeneity and structural quality was examined by a high-resolution SEM microscope (QUANTA FEG 650). The FESEM was operated in low vacuum mode a 20 kV with large field detector (LFD). Morphology was analysed before and after nanofiltration tests to evaluate membrane integrity maintenance.

To determine the nanofiltration performance, 100 ml of 10 mg/l of MB was passed through each of the fabricated membranes to calculate their rejection and permeation flux. An average rejection and flux of the three membranes of each type was obtained and the standard deviation was respectively recorded.

Results and discussion

3.1 Membrane morphology and thickness at changing GO and PPD concentrations

Images of the assembled membranes at their respective GO and crosslinker concentrations are displayed in Figure 1. Darkening in membrane pigmentation at heightening GO concentration is evident and further confirmed by means of FESEM (Figure 2). Good membrane continuity and structural integrity can be corroborated from the images.

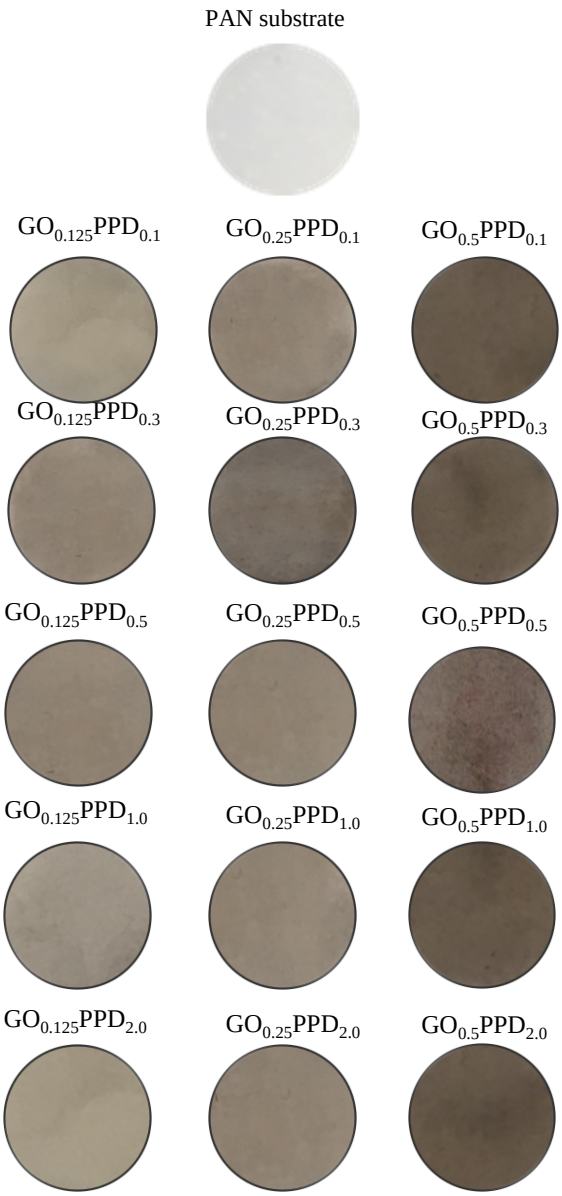

Figure 1. *Images of the membranes at different GO and PPD concentrations.*

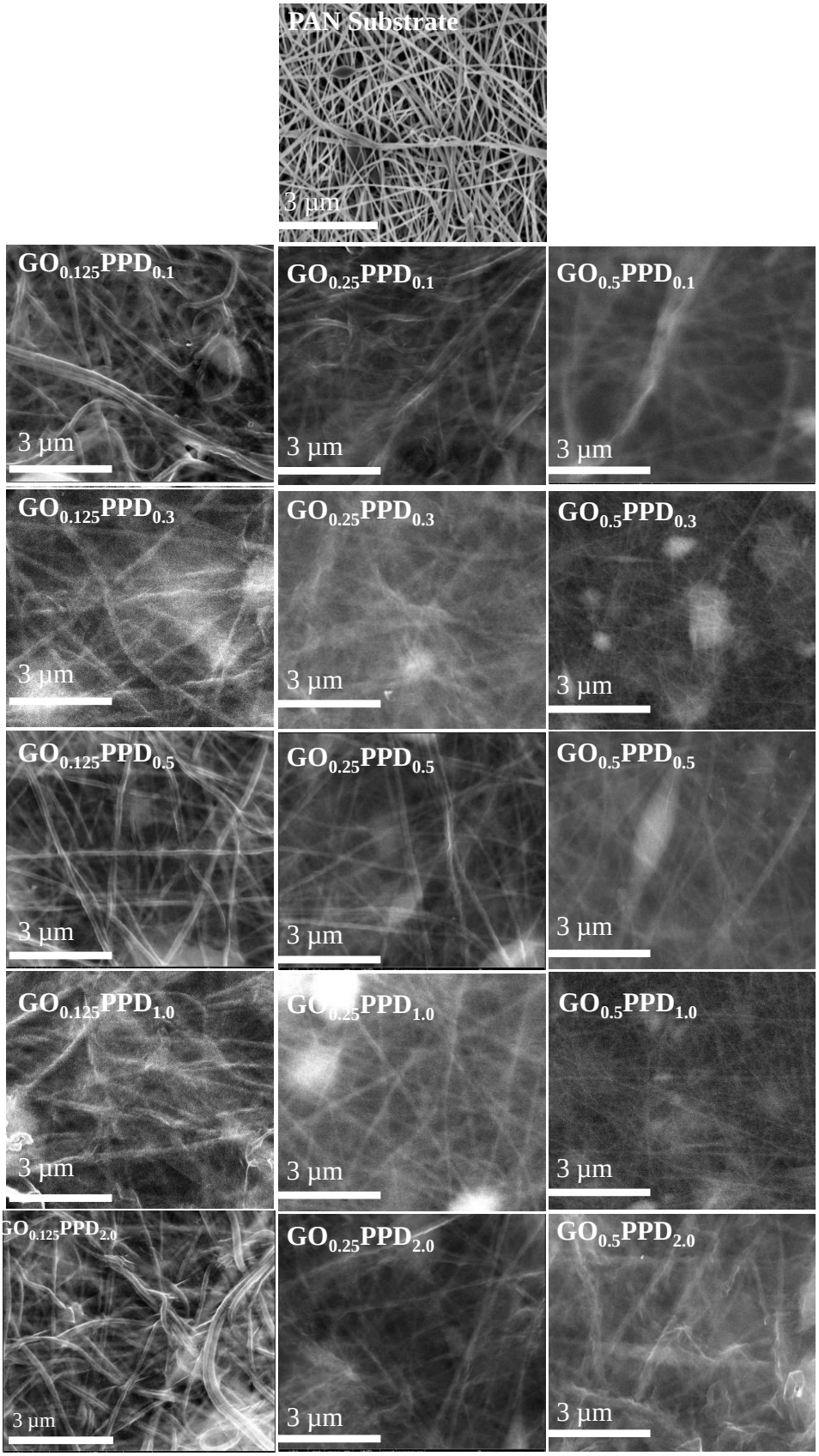

Figure 2. *FESEM images of the fabricated membranes.*

From the FESEM images, it is observable that an increase in GO concentration improves the covering of the PAN substrates by the nanosheets owing to GO intra-connections [30]. This is evidenced in the lessening visibility of the fibres of the PAN support filters (Figure 2). For the crosslinker PPD however, change in its concentration is not very noticeable on membrane morphology, which is mostly governed by GO as a result of its large surface area [31,32].

Measurements by means of stylus profilometry suggest that thickness primarily depends on the concentration range of GO. Increasing the concentration of GO while keeping that of the crosslinker constant results in a notable rise in the nanomeric thickness (Table 1). For example, fixing PPD concentration at 1.0 mg/ml, 2.1 nm thick film is recorded at a GO concentration of 0.125 mg/ml, while the thickness reaches a value of 5.9 nm if the concentration of GO is risen to 0.5 mg/ml (Table 1). This is inherently tied to the higher *intra*-interaction between GO nanosheets via dipole – dipole, van der Waal's forces, hydrogen bonding and $\pi - \pi$ stacking [33] resulting in multiple layers being attached at each assembly cycles [34]. On the contrary, keeping GO concentration constant while increasing that of PPD from 0.1 mg/ml to 2.0 mg/ml results in a minimal change in thickness of only up to 1.6 nm (Table 1).

Table 1. *Thickness of relative thin films at varying concentrations.*

Membrane	**Average thickness (nm)**
$GO_{0.125}PPD_{0.1}$	1.1 ± 1.4
$GO_{0.125}PPD_{0.3}$	1.4 ± 1.3
$GO_{0.125}PPD_{0.5}$	1.9 ± 1.2
$GO_{0.125}PPD_{1.0}$	2.1 ± 1.4
$GO_{0.125}PPD_{2.0}$	2.2 ± 0.8
$GO_{0.25}PPD_{0.1}$	3.7 ± 1.1
$GO_{0.25}PPD_{0.3}$	3.4 ± 0.5
$GO_{0.25}PPD_{0.5}$	3.9 ± 0.6
$GO_{0.25}PPD_{1.0}$	4.0 ± 0.6
$GO_{0.25}PPD_{2.0}$	4.2 ± 0.4
$GO_{0.5}PPD_{0.1}$	4.6 ± 0.8
$GO_{0.5}PPD_{0.3}$	5.7 ± 0.8
$GO_{0.5}PPD_{0.5}$	6.1 ± 0.4
$GO_{0.5}PPD_{1.0}$	5.9 ± 0.3
$GO_{0.5}PPD_{2.0}$	6.2 ± 0.4

3.2 The impact of varying concentration on nanofiltration

The nanofiltration results show a positive correlative relation between GO concentration and performance in terms of nanofiltration efficiency (Table 2). This is advocated to the lengthening of membrane tortuosity with GO accumulation, which is backed by the pictures shown in Figure 1, the micrographs in Figure 2, as well as the thickness characterisations (Table 1). Increasing the GO load from 0.125 mg/ml to 0.5 mg/ml while keeping the crosslinker concentration constant result in an average increment of 20.5% in MB rejection (Table 2). A greater presence of GO sheets benefits the selective permeation and adsorption of MB via $\pi - \pi$ interactions [35,36] and therefore a higher rejection rate [37,38]. Moreover, high GO concentration also comes with high membrane hydrophilicity and accordingly wettability along with reduced anti-fouling [24,39,40].

Table 2. *Nanofiltration performance, rejection, and permeation flux results.*

	Rejection (%)	**Flux (l/m^2.h)**
$GO_{0.125}PPD_{0.1}$	74.6 ± 2.1	29.5 ± 3.5
$GO_{0.125}PPD_{0.3}$	74.6 ± 3.7	26.2 ± 2.8
$GO_{0.125}PPD_{0.5}$	75.4 ± 2.3	25.2 ± 2.3
$GO_{0.125}PPD_{1.0}$	76.9 ± 3.3	25.2 ± 1.7
$GO_{0.125}PPD_{2.0}$	77.7 ±1.9	24.7 ± 2.1
$GO_{0.25}PPD_{0.1}$	87.7 ± 2.4	18.5 ± 1.9
$GO_{0.25}PPD_{0.3}$	91.2 ± 2.1	17.2 ± 1.6
$GO_{0.25}PPD_{0.5}$	91.7 ± 1.3	16.2 ± 1.3
$GO_{0.25}PPD_{1.0}$	91.3 ± 1.1	16.5 ± 1.8
$GO_{0.25}PPD_{2.0}$	91.4 ± 0.7	15.7 ± 0.9
$GO_{0.5}PPD_{0.1}$	94.4 ± 1.0	9.3 ± 1.6
$GO_{0.5}PPD_{0.3}$	95.0 ± 0.8	6.0 ± 1.1
$GO_{0.5}PPD_{0.5}$	97.9 ± 0.4	4.6 ± 0.9
$GO_{0.5}PPD_{1.0}$	98.0 ± 0.3	4.4 ± 0.5
$GO_{0.5}PPD_{2.0}$	98.3 ± 0.4	3.9 ± 1.4

The positive impact of PPD concentration on membrane rejection rate is promoted by the high crosslinking degree of the membranes. As the crosslinker concentration increases, the quantity of interconnected GO nanosheets is likely to be more, resulting in reduced membrane swelling and therefore enhanced performance [41]. However, the crosslinker beneficial influence seems to stagnate

when reaching a certain concentration. In fact, membrane rejection shows a plateau at approx. 1:1 GO:PPD ratio. This is especially evident at GO concentrations of 0.25 and 0.5 mg/ml (Table 2). For instance, at 0.25 mg/ml of GO little variation in rejection from 91.2 to 91.4% is noticed, although the crosslinker concentration increases from 0.3 to 2.0 mg/ml. A similar trend is observed at 0.5 mg/ml of GO where the rejection rate slightly changes from 97.7 to 98.3% as the crosslinker concentration rises from 0.5 mg/ml to 2.0 mg/ml. Thus, to further evaluate the role of PPD concentration on membrane stability and performance, membranes fabricated with the 0.5 mg/ml GO suspension were selected for characterisation by means of XPS (Table 3).

Table 3. *Surface chemistry of the membranes fabricated with a 0.5 mg/ml GO suspension and different concentrations of PPD (0.1, 0.3, 0.5, 1.0, 2.0 mg/ml).*

	$GO_{0.5}PPD_{0.1}$	$GO_{0.5}PPD_{0.3}$	$GO_{0.5}PPD_{0.5}$	$GO_{0.5}PPD_{1.0}$	$GO_{0.5}PPD_{2.0}$
C1s (at.%)	77.6	77.2	73.9	74.0	69.3
O1s (at.%)	19.3	18.2	19.9	19.9	23.4
N1s (at.%)	3.1	4.6	6.2	6.2	7.3
N/C	0.0401	0.0596	0.0842	0.0833	0.1053
Csp^2+Csp^3 (%)	60.3	65.7	63.9	63.3	61.7
C(epoxy)/C-OH/C=N (%)	28.7	22.0	21.2	21.7	20.9
C=O/C-N (%)	7.7	6.1	8.7	9.0	9.3
COOH (%)	3.3	3.7	6.2	5.9	6.7
π-π* (%)	0.0	2.4	0.0	0.1	1.4

In general, nitrogen content increases with PPD concentration from 3.1% up to 7.3% (Table 3). However, it seems that the rises in nitrogen percentage are more significant when PPD quantity range from 0.1 mg/ml to 0.5 mg/ml. Successive upsurges in PPD concentration are not as effective in incorporating nitrogen onto the surface of the membranes. The reaction mechanism between GO and PPD takes place via an epoxy ring opening reaction [22] where the primary amines present on PPD are converted to secondary amines and new C-N bonds are also created [21,22]. This is in agreement with the XPS results shown in Table 3, where it is noted a reduction in the epoxy groups (from 28.7% to 20.9%) and a rise in the C-N content (from 7.7% to 9.3%) when the concentration of PPD increases from 0.1 mg/ml up to 2 mg/ml. However, it appears that a concentration of 0.5 mg/ml of PPD is

sufficient to deal with most of the epoxy groups present on the GO surface, as its percentage remains invariable with higher PPD additions (21.2% vs 20.9% with 0.5 mg/ml and 2.0 mg/ml of PPD respectively, Table 3). This suggests that the crosslinking degree provided by a ratio 1:1 GO:PPD efficiently interconnects the GO nanosheets and therefore an excess of PPD does not offer further improvement on membrane performance.

An increase in GO and crosslinker concentrations has a reciprocal impact onto the permeation flux as a result of lengthening membrane tortuosity due to GO and enhanced intactness from crosslinking (Table 2) [41,42].

3.3 Impact of crosslinking concentration on membrane stability and performance

The role of the diamine crosslinker in influencing GO membrane stability and intactness was studied by FESEM. Membranes prepared with the GO suspension of 0.5 mg/ml were also observed under FESEM after the nanofiltration experiments, and once they were completely dried, to verify the extent of membrane integrity maintenance at varying crosslinker concentration.

At a GO:PPD ratio of less than 1, micro-cracking of the membranes is clearly observable (Figure 3). At lower concentrations, fewer crosslinker molecules are expected to hold the nanosheets together, hence the detected dry-infused cracking, which impacts on membrane operation. On the contrary with concentrations of PPD equal or higher than 0.5 mg/ml more nanosheets are being held together and thus improved structural intactness with no cracks spotted (Figure 3).

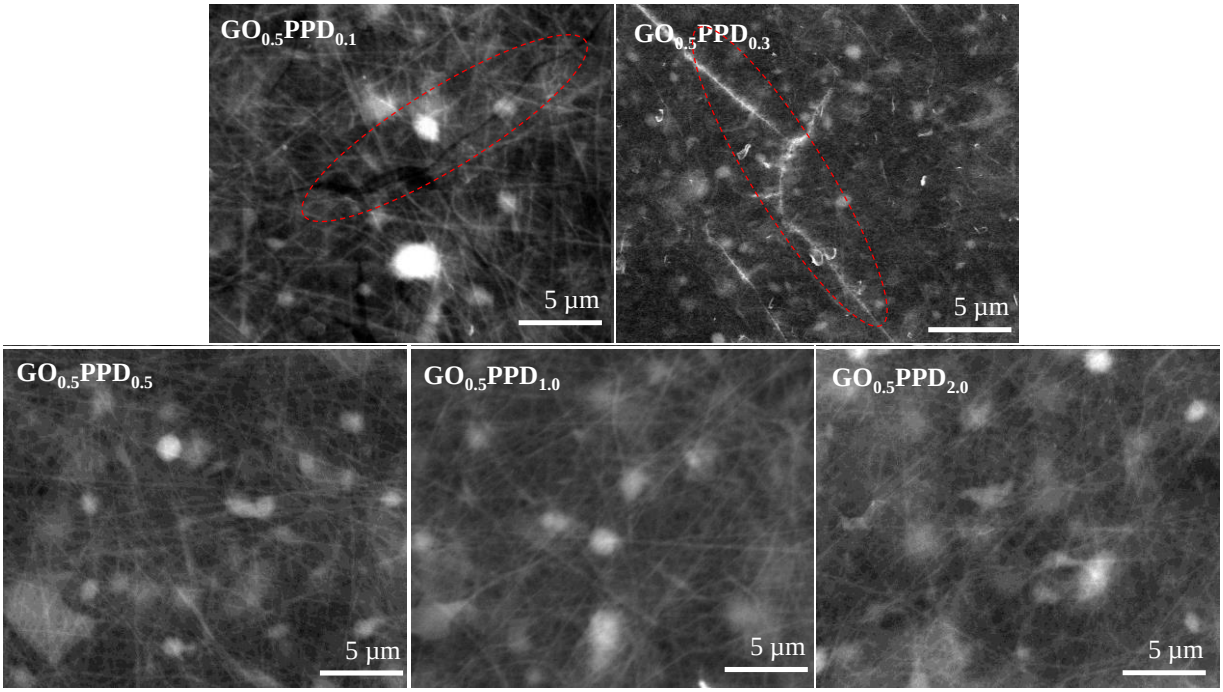

Figure 3. *SEM images of crosslinked membranes with 0.5 mg/ml of GO post nanofiltration.*

The enhancement in nanofiltration performance with crosslinker concentration can thus be backed by the better membrane intactness and stability instigated by PPD. Conclusively, basing on the separation results and the stability maintenance post nanofiltration, a GO:PPD 1:1 ratio is commendable to achieve excellent performance and improved membrane stability.

4. Conclusions

This work investigates the influence of concentration of GO and PPD on the fabrication of crosslinked water purification membranes with special emphasis on membrane morphology, thickness, structural intactness and nanofiltration performance. Rejection rates are notably improved with GO concentration, and PPD is also crucial due to its role interconnecting GO nanosheets and therefore avoiding membrane swelling. However, PPD concentration seems to be critical up to a GO:PPD ratio of 1:1, since above this ratio membrane rejection shows a plateau. This may be related to the nitrogen content incorporated onto the membranes via epoxy ring opening reactions. There is a reduction in the epoxy groups and an increment on the C-N groups when PPD concentration rises from 0.1 mg/ml to

0.5 mg/ml. Nevertheless, at higher PPD concentrations those functional groups keep relatively constant, which suggests that a GO:PPD ratio of 1:1 effectively crosslink the GO nanosheets.

Acknowledgements

The authors are grateful to the Botswana Government's Top Achievers Scholarship Programme for offering a financial Scholarship (TR. 163096) that aided the carrying out of this work. Authors also thank HarwellXPS EPSRC National Facility for the XPS characterisations. SM-E would like to express her gratitude for the Fellowship supported by the Royal Academy of Engineering under the Leverhulme Trust Research Fellowships scheme (LTRF2021\17130).

References

[1] R.I. McDonald, P. Green, D. Balk, B.M. Fekete, C. Revenga, M. Todd, M. Montgomery, Urban growth, climate change, and freshwater availability, Proc. Natl. Acad. Sci. U. S. A. 108 (2011) 6312–6317. https://doi.org/10.1073/pnas.1011615108.

[2] Y. Wada, L.P.H. Van Beek, M.F.P. Bierkens, Modelling global water stress of the recent past : on the relative importance of trends in water demand and climate variability, Hydrol. Earth Syst. Sci. 15 (2011) 3785–3808. https://doi.org/10.5194/hess-15-3785-2011.

[3] V. Kandjou, D.O. Nkwe, F. Ntuli, N. Keroletswe, Evaluating the degree of chemical contamination of underground aquifers in Botswana and analysing viable purification and desalination means; a review, Chem. Eng. Res. Des. (2022). https://doi.org/https://doi.org/10.1016/j.cherd.2022.03.055.

[4] M.R. Esfahani, S.A. Aktij, Z. Dabaghian, M.D. Firouzjaei, A. Rahimpour, J. Eke, I.C. Escobar, M. Abolhassani, L.F. Greenlee, A.R. Esfahani, A. Sadmani, N. Koutahzadeh, Nanocomposite membranes for water separation and purification: Fabrication, modification, and applications, Sep. Purif. Technol. 213 (2019) 465–499. https://doi.org/10.1016/j.seppur.2018.12.050.

[5] Z. Yang, Y. Zhou, Z. Feng, X. Rui, T. Zhang, Z. Zhang, A review on reverse osmosis and nanofiltration membranes for water purification, Polymers (Basel). 11 (2019) 1–22. https://doi.org/10.3390/polym11081252.

[6] R.K. Joshi, S. Alwarappan, M. Yoshimura, V. Sahajwalla, Y. Nishina, Graphene oxide: The new membrane material, Appl. Mater. Today. 1 (2015) 1–12. https://doi.org/10.1016/j.apmt.2015.06.002.

[7] C.A.. Siskens, Chapter 13 Applications of ceramic membranes in liquid filtration, Membr. Sci. Technol. 4 (1996) 619–639. https://www.sciencedirect.com/science/article/abs/pii/S0927519396800167.

[8] A.. Geim, K.. Novoselov, The rise of graphene, Nat. Mater. 3 (2007) 183–191. https://doi.org/10.1038/nmat1849.

[9] S.P. Surwade, S.N. Smirnov, I. V. Vlassiouk, R.R. Unocic, G.M. Veith, S. Dai, S.M. Mahurin, Water desalination using nanoporous single-layer graphene, Nat. Nanotechnol. 10 (2015) 459–464. https://doi.org/10.1038/nnano.2015.37.

[10] C.J. Russo, J.A. Golovchenko, Atom-by-atom nucleation and growth of graphene nanopores, Proc. Natl. Acad. Sci. 109 (2012) 5953–5957. https://doi.org/10.1073/pnas.1119827109.

[11] S.C. O'Hern, C.A. Stewart, M.S.H. Boutilier, J.C. Idrobo, S. Bhaviripudi, S.K. Das, J. Kong, T. Laoui, M. Atieh, R. Karnik, Selective molecular transport through intrinsic defects in a single layer of CVD graphene, ACS Nano. 6 (2012) 10130–10138. https://doi.org/10.1021/nn303869m.

[12] R.. Nair, H.. Wu, A. V. Jayaram, V. Grigorieva, A.. Geim, Unimpeded Permeation of Water Through Helium-Leak–Tight Graphene-Based Membranes, Science (80-.). 335 (2012) 442–445. https://doi.org/10.1126/science.1211694.

[13] D.A. Dikin, S. Stankovich, E.J. Zimney, R.D. Piner, G.H.B. Dommett, G. Evmenenko, S.T. Nguyen, R.S. Ruoff, Preparation and characterization of graphene oxide paper, Nature. 448 (2007) 457–460. https://doi.org/10.1038/nature06016.

[14] Y. Han, Z. Xu, C. Gao, Ultrathin graphene nanofiltration membrane for water purification, Adv. Funct. Mater. 23 (2013) 3693–3700. https://doi.org/10.1002/adfm.201202601.

[15] D. Li, M.. Mueller, S. Gilje, R.. Kaner, G.. Wallace, Processable aqueous dispersions of graphene nanosheets, Nat. Nanotechnol. 3 (2008) 101–108. https://www.nature.com/articles/nnano.2007.451.

[16] D.W. Johnson, B.P. Dobson, K.S. Coleman, A manufacturing perspective on graphene dispersions, Curr. Opin. Colloid Interface Sci. 20 (2015) 367–382. https://doi.org/10.1016/j.cocis.2015.11.004.

[17] S. Zheng, Q. Tu, J.J. Urban, S. Li, B. Mi, Swelling of Graphene Oxide Membranes in Aqueous Solution: Characterization of Interlayer Spacing and Insight into Water Transport Mechanisms, ACS Nano. 11 (2017) 6440–6450. https://doi.org/10.1021/acsnano.7b02999.

[18] Y. Mo, X. Zhao, Y. xiao Shen, Cation-dependent structural instability of graphene oxide membranes and its effect on membrane separation performance, Desalination. 399 (2016) 40–46. https://doi.org/10.1016/j.desal.2016.08.012.

[19] L. Huang, J. Chen, T. Gao, M. Zhang, Y. Li, L. Dai, L. Qu, G. Shi, Reduced Graphene Oxide Membranes for Ultrafast Organic Solvent Nanofiltration, Adv. Mater. 28 (2016) 8669–8674. https://doi.org/10.1002/adma.201601606.

[20] J. Abraham, K.S. Vasu, C.D. Williams, K. Gopinadhan, Y. Su, C.T. Cherian, J. Dix, E. Prestat, S.J. Haigh, I. V. Grigorieva, P. Carbone, A.K. Geim, R.R. Nair, Tunable sieving of ions using graphene oxide membranes, Nat. Nanotechnol. 12 (2017) 546–550.

https://doi.org/10.1038/nnano.2017.21.

[21] V. Kandjou, A.M. Perez-mas, B. Acevedo, M. Hernaez, A.G. Mayes, S. Melendi-espina, Enhanced covalent p-phenylenediamine crosslinked graphene oxide membranes : Towards superior contaminant removal from wastewaters and improved membrane reusability, J. Hazard. Mater. 380 (2019) 120840. https://doi.org/10.1016/j.jhazmat.2019.120840.

[22] V. Kandjou, M. Hernaez, B. Acevedo, S. Melendi-espina, Interfacial crosslinked controlled thickness graphene oxide thin- fi lms through dip-assisted layer-by-layer assembly means, Prog. Org. Coatings. 137 (2019). https://doi.org/10.1016/j.porgcoat.2019.105345.

[23] V. Kandjou, Z. Gonzalez, B. Acevedo, J.M. Munuera, J.I. Paredes, S. Melendi-espina, Influence of graphene oxide's characteristics on the fabrication and performance of crosslinked nanofiltration membranes, J. Taiwan Inst. Chem. Eng. 000 (2021) 1–8. https://doi.org/10.1016/j.jtice.2021.01.023.

[24] S. Bala, D. Nithya, M. Doraisamy, Exploring the effects of graphene oxide concentration on properties and antifouling performance of PEES / GO ultrafiltration membranes, High Perform. Polym. 30 (2018) 375–383. https://doi.org/10.1177/0954008317698547.

[25] C. Zhao, X. Xu, J. Chen, F. Yang, Effect of graphene oxide concentration on the morphologies and antifouling properties of PVDF ultrafiltration membranes, J. Environ. Chem. Eng. 1 (2013) 349–354. https://doi.org/10.1016/j.jece.2013.05.014.

[26] P.L. Mores, A.M. Arias, N.J. Scenna, J.A. Caballero, S.F. Mussati, M.C. Mussati, Membrane-based processes: Optimization of hydrogen separation by minimization of power, membrane area, and cost, Processes. 6 (2018). https://doi.org/10.3390/pr6110221.

[27] A.P. Dementjev, A. de Graaf, M.C.. van de Sanden, A.. Maslakov, K.I Naumkin, A.. Serov, X-Ray photoelectron spectroscopy reference data for identification of the C3 N4 phase in

carbon-nitrogen films., Diam. Relat. Mater. 9 (2000) 1904–1907. https://doi.org/10.1016/S0925-9635(00)00345-9.

[28] S. Bhattacharyya, C. Cardinaud, G. Turban, Spectroscopic determination of the structure of amorphous nitrogenated carbon films, J. Appl. Phys. 83 (1998) 4491.

[29] S. Bhattacharyya, J. Hong, G. Turban, Determination of the structure of amorphous nitrogenated carbon films by combined Raman and x-ray photoemission spectroscopy, J. Appl. Phys. 83 (1998) 3917. https://doi.org/10.1063/1.367312.

[30] E.A. Chiticaru, L. Pilan, C.M. Damian, E. Vasile, J.S. Burns, M. Ionita, Influence of graphene oxide concentration when fabricating an electrochemical biosensor for DNA detection, Biosensors. 9 (2019) 1–18. https://doi.org/10.3390/bios9040113.

[31] A. Lerf, H. He, M. Forster, J. Klinowski, Structure of Graphite Oxide Revisited [I], J. Phys. Chem. B. 102 (1998) 4477–4482. https://doi.org/10.1021/jp9731821.

[32] D.R. Dreyer, S. Park, C.W. Bielawski, R.S. Ruoff, The chemistry of graphene oxide, R. Soc. Chem. 39 (2010) 228–240. https://doi.org/10.1039/b917103g.

[33] V. Georgakilas, J.N. Tiwari, K.C. Kemp, A.B. Perman, Jason A. Bourlinos, K.S. Kim, R. Zboril, Noncovalent Functionalization of Graphene and Graphene Oxide for Energy Materials, Biosensing, Catalytic, and Biomedical Applications, Chem. Rev. 116 (2016) 5464–5519. https://doi.org/10.1021/acs.chemrev.5b00620.

[34] J. Yan, J. Liu, Z. Fan, T. Wei, L. Zhang, High-performance supercapacitor electrodes based on highly corrugated graphene sheets, Carbon N. Y. 50 (2012) 2179–2188. https://doi.org/10.1016/j.carbon.2012.01.028.

[35] W. Zhang, C. Zhou, W. Zhou, A. Lei, Q. Zhang, Q. Wan, B. Zou, Fast and considerable adsorption of methylene blue dye onto graphene oxide, Bull. Environ. Contam. Toxicol. 87

(2011) 86–90. https://doi.org/10.1007/s00128-011-0304-1.

[36] B. Zhang, Y. Li, T. Wu, D. Sun, W. Chen, X. Zhou, Magnetic iron oxide/graphene oxide nanocomposites: Formation and interaction mechanism for efficient removal of methylene blue and p-tert-butylphenol from aqueous solution, Mater. Chem. Phys. 205 (2018) 240–252. https://doi.org/10.1016/j.matchemphys.2017.11.015.

[37] N.S. Kaya, A. Yadav, M. Wehrhold, L. Zuccaro, K. Balasubramanian, Binding Kinetics of Methylene Blue on Monolayer Graphene Investigated by Multiparameter Surface Plasmon Resonance, ACS Omega. 3 (2018) 7133–7140. https://doi.org/10.1021/acsomega.8b00689.

[38] C.R. Minitha, M. Lalitha, Y.L. Jeyachandran, L. Senthilkumar, R.T. Rajendra Kumar, Adsorption behaviour of reduced graphene oxide towards cationic and anionic dyes: Co-action of electrostatic and π – π interactions, Mater. Chem. Phys. 194 (2017) 243–252. https://doi.org/10.1016/j.matchemphys.2017.03.048.

[39] H. Karkhanechi, R. Takagi, H. Matsuyama, Biofouling resistance of reverse osmosis membrane modified with polydopamine, Desalination. 336 (2014) 87–96. https://doi.org/10.1016/j.desal.2013.12.033.

[40] J.H. Li, X.S. Shao, Q. Zhou, M.Z. Li, Q.Q. Zhang, The double effects of silver nanoparticles on the PVDF membrane: Surface hydrophilicity and antifouling performance, Appl. Surf. Sci. 265 (2013) 663–670. https://doi.org/10.1016/j.apsusc.2012.11.072.

[41] W.S. Hung, C.H. Tsou, M. De Guzman, Q.F. An, Y.L. Liu, Y.M. Zhang, C.C. Hu, K.R. Lee, J.Y. Lai, Cross-linking with diamine monomers to prepare composite graphene oxide-framework membranes with varying d-spacing, Chem. Mater. 26 (2014) 2983–2990. https://doi.org/10.1021/cm5007873.

[42] R.K. Bharadwaj, Modeling the barrier properties of polymer-layered silicate nanocomposites,

Macromolecules. 34 (2001) 9189–9192. https://doi.org/10.1021/ma010780b.